Design for Reliability and Robustness Tool Platform for Power Electronic Systems – Study Case on Motor Drive Applications

Ionuț Vernica, Huai Wang, and Frede Blaabjerg
Department of Energy Technology, Aalborg University
Pontoppidanstræde 101, 9220 Aalborg Øst, Denmark
Email: iov@et.aau.dk, hwa@et.aau.dk, and fbl@et.aau.dk

***Abstract*—Because of the high cost of failure, the reliability performance of power semiconductor devices is becoming a more and more important and stringent factor in many energy conversion applications. Thus, the need for appropriate reliability analysis of the power electronics emerges. Due to its conventional approach, mainly based on failure statistics from the field, the reliability evaluation of the power devices is still a challenging task. In order to address the given problem, a MATLAB based reliability assessment tool has been developed. The Design for Reliability and Robustness (DfR^2) tool allows the user to easily investigate the reliability performance of the power electronic components (or sub-systems) under given input mission profiles and operating conditions. The main concept of the tool and its framework are introduced, highlighting the reliability assessment procedure for power semiconductor devices. Finally, a motor drive application is implemented and the reliability performance of the power devices is investigated with the help of the DfR^2 tool, and the resulting reliability metrics are presented.**

***Index Terms*—Reliability tool, power semiconductor device, system-level reliability, motor drive system.**

I. Introduction

Power electronics are being widely used in many mission-critical applications such as renewable power generation, power transmission, traction applications or motor drives, and due to their essential role within power systems, the reliability of the power converter is one of the main factors that influences the overall efficiency and cost of the system.

However, according to [1]-[5], the power electronic converter represents one of the most fragile sub-systems in terms of reliability. In [1], based on the failure information and field statistics from a photovoltaic plant operated throughout the course of 5 years, it has been concluded that the inverter is the most critical sub-assembly of the system. Furthermore, in [2]-[4] it has been found that the frequency converter represents one of the most prone to failure sub-systems of the wind turbine system. A similar conclusion has been drawn in [5], where the inverter unit contributed with 65% to the failure rate of a motor drive system.

Consequently, in order to understand the main causes behind the high failure rates in power converters, an in-depth component-level reliability survey has been carried out in [6], and it has been concluded that the power devices and the capacitors represent the most fragile components, with respect to reliability.

According to [7], [8], the high probability of failure in the power devices is primarily due to the thermal cycling which occurs in the device. These adverse temperature swings are mainly caused by the fluctuating load of the converter or environmental temperature variations, and thus leading to some of the most common failure mechanisms, such as bond wire lift-off or solder cracks [9], [10]. As a result, the unexpected wear-out failures of the power electronic components will lead to an increase in maintenance cost, and a cutback in the total energy production of the system (due to downtime), and thus resulting in a higher cost of energy conversion.

Unfortunately, the conventional reliability improvement approach of power converters is still mainly based on the failure information and statistics from the field. Due to the fact that this method is expensive and time consuming, the need for prior reliability assessment, during the design and development phase, arises. Thus, by introducing a reliability evaluation tool within the initial phases of the product life cycle, the weaknesses and lifetime of the power converter can be identified before introducing the product into the market. Thus, the proposed DfR^2 tool will help to optimize the design of the power converter in order to achieve a better balance between reliability and cost, and finally result in a significant cost reduction in the whole lifetime cycle of the product.

Similar reliability assessment tool concepts have been proposed in recent years, such as Sherlock Automated Design Analysis [11], or Simulation Assisted Reliability Assessment (SARA) [12]. Although the previously mentioned software tools are capable of analyzing the reliability performance of the electronic components either through physics-to-failure models or through reliability statistics data, they are manly focused on microelectronics systems, and do not take into consideration the real-life operating mission profiles of the system.

Moreover, in [13] and [14] an initial reliability assessment tool has been proposed and its main concept and features have been introduced. Despite its many advantages, such as integrating a relatively complex structure under a user-friendly and easy-to-use interface, some crucial drawbacks were present, among which: lack of modularity, reliability analysis feature only for power semiconductor devices, or the absence of system-level reliability investigation.

978-1-5386-1180-7/18/$31.00 ©2018 IEEE

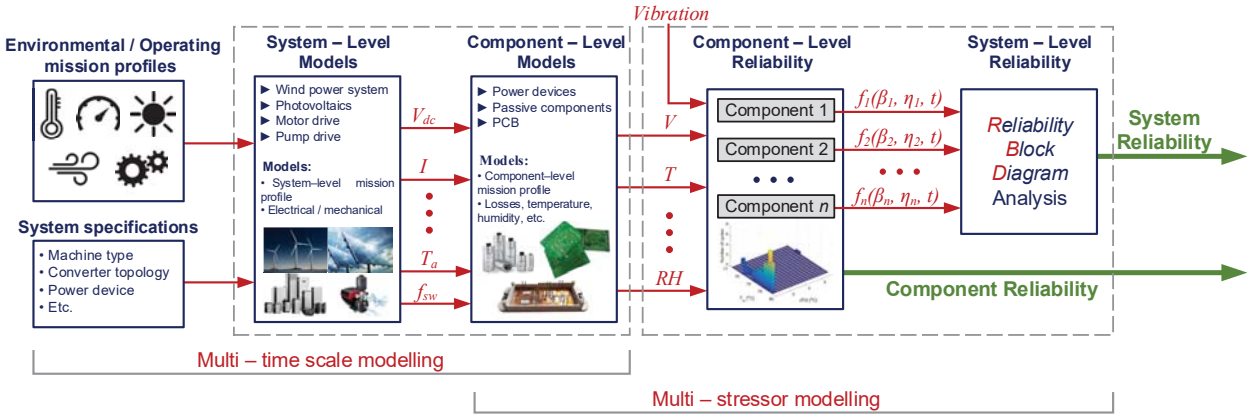

Fig. 1. General structure and flow of the DfR^2 tool platform.

Therefore, in this paper a novel reliability assessment tool platform focused solely on power electronic systems, which aims at addressing the previously mentioned issues, is proposed. The main concept of the tool, together with its framework and functionality are initially described. Finally, in order to highlight the reliability assessment process for the power semiconductor devices, a motor drive application study case is investigated and the resulting reliability metrics on component/system-level are presented.

II. Design for Reliability and Robustness Tool Framework

The Design for Reliability and Robustness (DfR^2) tool has been developed in order to assist the reliability performance investigation of power electronics components (e.g. semiconductor devices, capacitors, etc.) in a fast and straightforward manner, and inherently help optimize the design and behavior of the power converter under given mission profiles and system specifications. The tool framework has been developed with a generic and modular approach, and thus allows for various power electronic application (e.g. wind power generation, photovoltaics, motor drives, etc.) to be implemented and analyzed.

Keeping in mind the modular approach of the tool, an application independent reliability assessment procedure has been proposed and presented in Fig. 1. As it can be seen in Fig. 1, the environmental/operating mission profiles, together with the system specifications will represent the inputs to the the DfR^2 tool. According to the system-level models of the selected application, the electro-mechanical dynamic behavior of the system will be investigated, and the mission profiles can be translated into the converter-level electrical loading.

Afterwards, the resulting converter-level mission profiles can be inputted into the component-level models, where the loss and thermal characterization of the components of interest will be taken into account. Based on the outputted component thermal loading and other external stressors (such as vibration or humidity), the reliability assessment procedure for the power components can be applied.

As shown in Fig. 1, the tool employs the multi-timescale modelling concept [15], which allows the integration of the different time-constant of the system, ranging from microseconds (e.g. device switching) to days (e.g. environmental temperature variations). By employing the multi-timescale modeling concept the long-term environmental mission profiles can be translated to the component-level mission profiles, and thus facilitating the reliability assessment of the components of interest. During the component-level reliability investigation the multi-stressor modeling concept is applied, which will allow for multiple external stressors (e.g. temperature, relative humidity, and vibration) to be taken into account, and thus

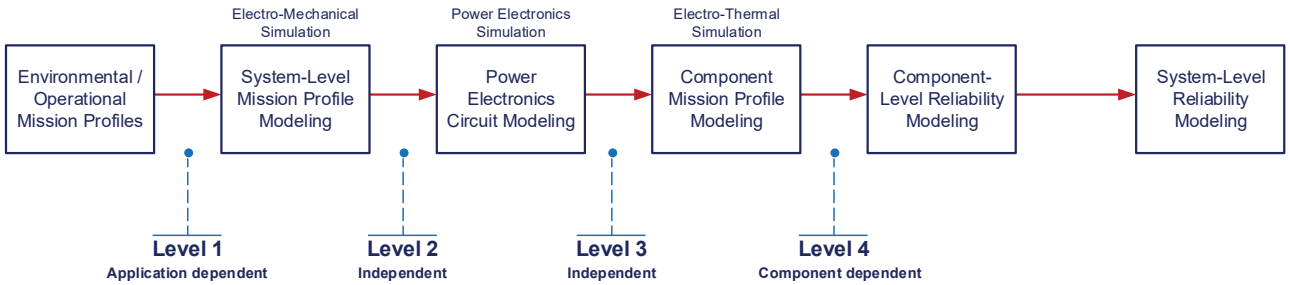

Fig. 2. Power device reliability assessment procedure for motor drive applications.

providing a more accurate lifetime estimation.

Due to its modular design concept, the DfR^2 tool will allow the user to select from different mission profile input levels, according to the available data. The reliability assessment procedure presented in Fig. 1 has been simplified and shown in Fig. 2 in order to highlight the different mission profile input levels, ranging from environmental to component-level, for a motor drive application.

As it can be noticed in Fig. 2, the environmental/operating mission profiles represent the Level 1 input level. This input level is application dependent, and thus the mission profiles will vary from one application to another. For the motor drive application study case that will be investigated within this paper, the required Level 1 mission profile consist of the ambient temperature profile (T_a), mechanical speed of the motor (ω_{mech}), and the load torque (T_{load}). Additionally, if the relative humidity is taken into consideration as a stressor for any of the components of interest, it can be included within the Level 1 mission profile inputs.

Level 2 and Level 3 mission profile inputs are application independent, and represent the system-level mission profiles, and converter-level mission profiles respectively.

The final mission profile input level available to the user is Level 4, which represents the component-level mission profiles. Similar to Level 1, this input level is component dependent, and thus the input mission profile will vary according to the selected component of interest. As shown in Fig. 2, the required Level 4 mission profiles for assessing the reliability of power device are the component voltage (V_{comp}), junction temperature (T_j), and case temperature (T_c).

Based on the component-level mission profile, the reliability performance of the power electronic component can be investigated. In case of the power devices, the component-level reliability assessment procedure begins with the processing of the mission profile data, which by means of counting algorithms (e.g. Rainflow counting) will represent the mission profile data so that it can be correctly applied to a lifetime model. After selecting the desired lifetime model (and adjusting its parameters if necessary), the B_x lifetime of the power devices can be estimated. The reliability assessment procedure ends by applying and taking into account the variations and uncertainties which may occur in the lifetime model coefficients, or stressor data.

At this point it should be noted that the reliability analysis is based mainly on the wear-out failure of the components, while the failures caused by random/catastrophic events will be taken into consideration as statistical user input data. Finally, the reliability information of each individual component is used in order to determine the reliability of the system (or subsystem), by means of Reliability Block Diagrams (RBD).

The DfR^2 tool has been designed based on MATLAB and Simulink. The reason for choosing MATLAB as the main software development platform, is due to its multitude of toolboxes and predefined functions, which will facilitate a faster implementation. In order to assure a user-friendly experience a Graphical User Interface (GUI) has been designed. The GUI will give the user various possibilities of interacting with the source code and simulation models employed within the tool, ranging from designing the system architecture (as shown in Fig. 3), modeling the power electronic components or

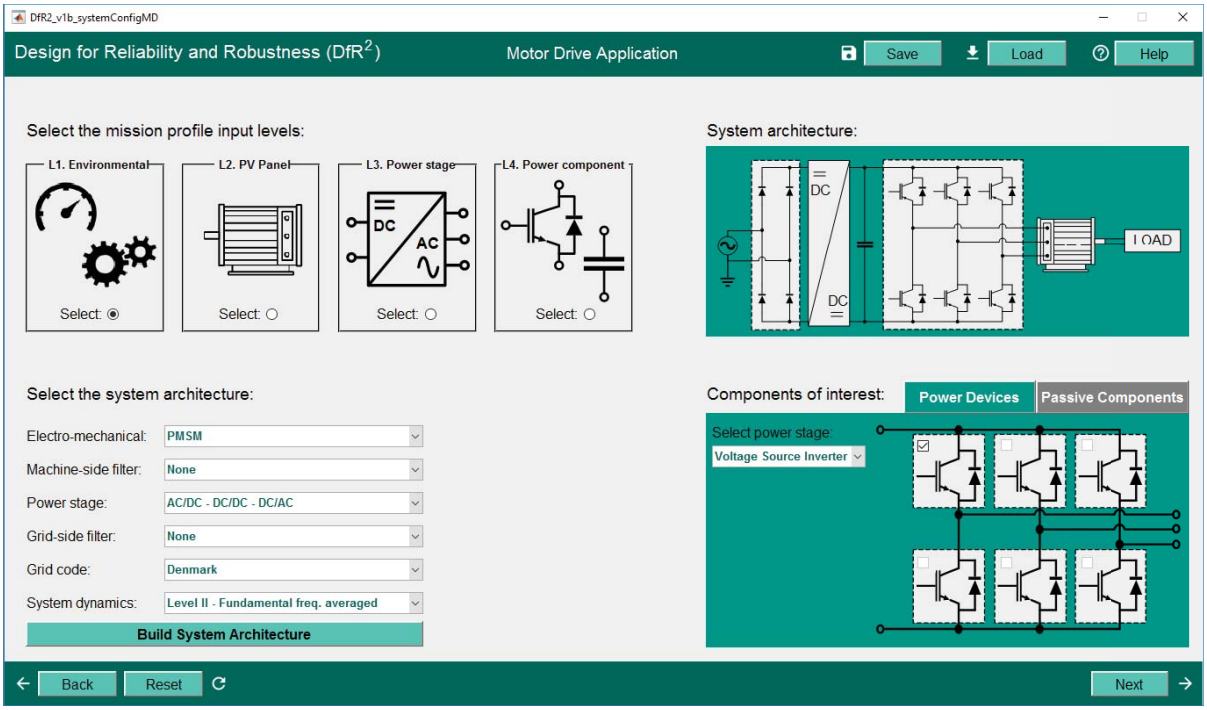

Fig. 3. "System Configuration" panel for the motor drive application of the DfR^2 tool.

visualizing and exporting the results in a fast an comprehensive manner. Moreover, in order to fulfill the imposed modularity requirements, the tool should be capable as acting as a plug-in to other 3rd party software. Thus, the user is given the option either to utilize the tool as a standalone software, or as a plug-in in connection with various programs focused on circuit simulation (e.g. PLECS, Saber, etc.), finite element simulation (e.g. ANSYS), or reliability (e.g. ReliaSoft).

III. Power Device Reliability Assessment in Motor Drive Systems

In order to validate the DfR^2 tool framework and its procedures, a motor drive application is selected as study case. Within this paper, the reliability investigation will be carried out only for the upper transistor/diode pair of phase A of the machine-side inverter, and it will follow the same procedure and flow as presented below.

A. System-level mission profile modeling

The motor drive system consists of a Permanent Magnet Synchronous Motor (PMSM), which is connected to the grid through a 2-level Voltage Source Inverter (VSI) on the machine side, and a single-phase PFC boost rectifier on the grid side, as shown in Fig. 4. The parameters of the motor drive system are shown in Table I, while the power module choice is a 30 A 600 V IGBT module.

The speed control of the motor is assured by means of Field Oriented Control (FOC), while the switching sequence of the power semiconductor devices of the converter is generated by a Space Vector Modulation (SVM) technique.

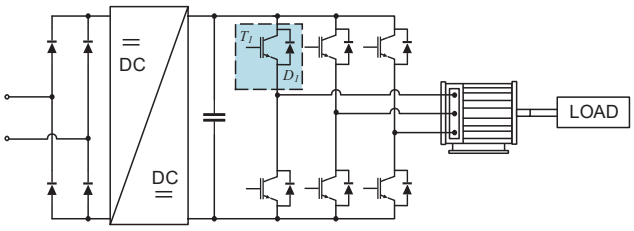

Fig. 4. Configuration of motor drive application with 3-phase inverter and PFC boost rectifier.

TABLE I. Parameters for study-case PMSM.

Parameter	Symbol	Value	Unit
Nominal Power	P_n	5000	[W]
Nominal Torque	T_n	24	[Nm]
Nominal Speed	ω_{mech}	2000	[rpm]
Maximum EMF	$V_{\text{EMF,max}}$	520	[V]
Rotor Inertia	J	0.0055	[Kgm^2]
Stator Resistance	R_s	0.39	[Ω]
Stator Inductance	L_s	4.9	[mH]
Nr. Pole Pairs	n_{pp}	4	[-]
DC-Link Voltage	V_{DC}	380	[V]
Switching Frequency	f_{sw}	10	[kHz]

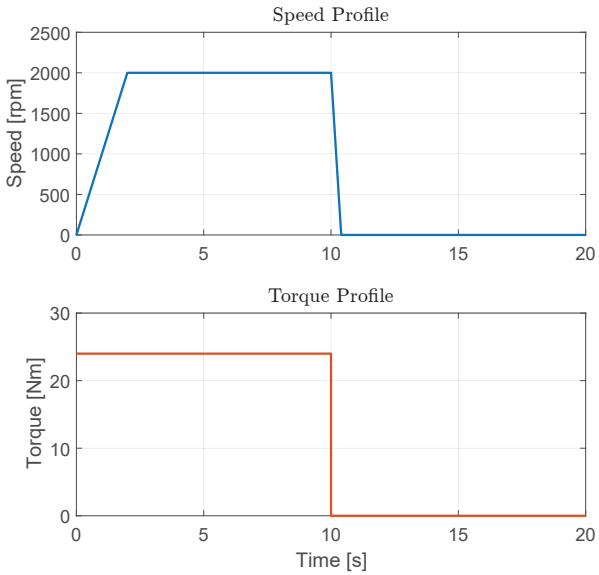

Fig. 5. Speed and torque mission profiles of the motor drive system (Operating mission profiles – Level 1).

The speed and torque mission profiles shown in Fig. 5 will represent the inputs to the system, and thus, according to Fig. 2, the level 1 mission profile input level is employed. Based on the electro-mechanical model of the PMSM, the current and voltage response of the machine can be determined, according to the given start-stop mission profiles and system specifications. The resulting current and voltage waveforms are presented in Fig. 6, and represent the system-level mission profiles (input level 2).

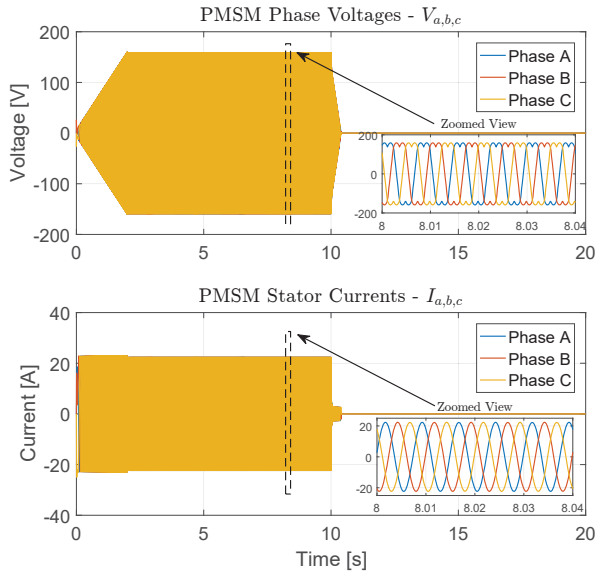

Fig. 6. Voltage and current loading of PMSM (System-level mission profiles – Level 2).

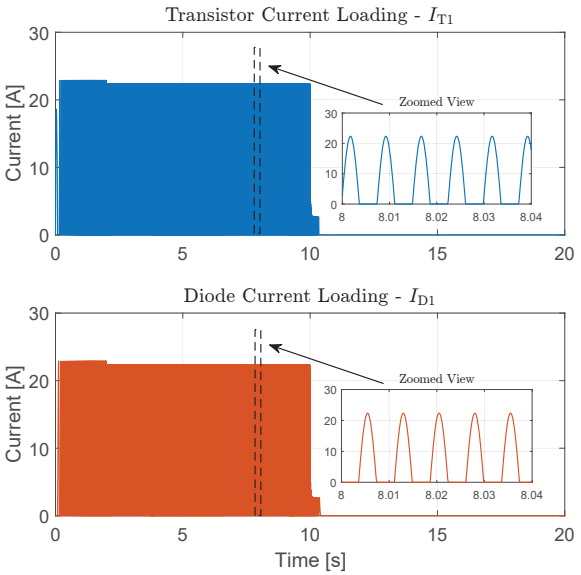

Fig. 7. Power device current loading (Converter-level mission profiles – Level 3).

B. Converter-level mission profile modeling

Afterwards, the system-level mission profiles can be translated into the converter-level mission profiles. According to the determined duty cycle, the current and voltage loading on each of the 6 transistors and 6 diodes can be identified. Therefore, the current which flows through of the upper transistor and diode from phase A of the machine-side VSI, are calculated and shown in Fig. 7. During the conduction period of the the devices, the voltage loading is equal to the DC-link voltage.

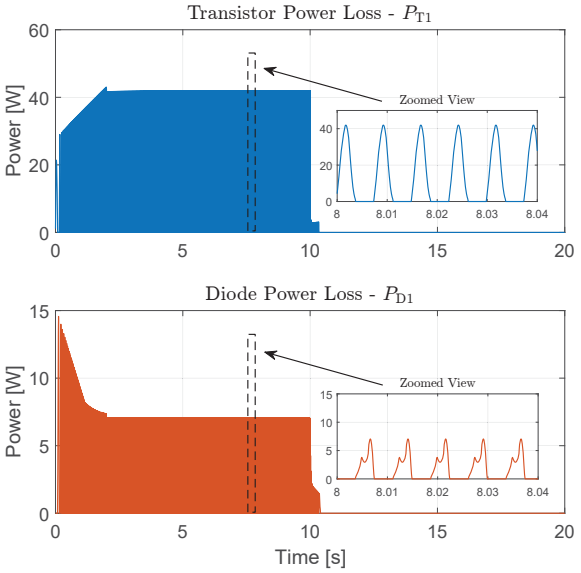

Fig. 8. Total power losses of the upper transistor/diode pair.

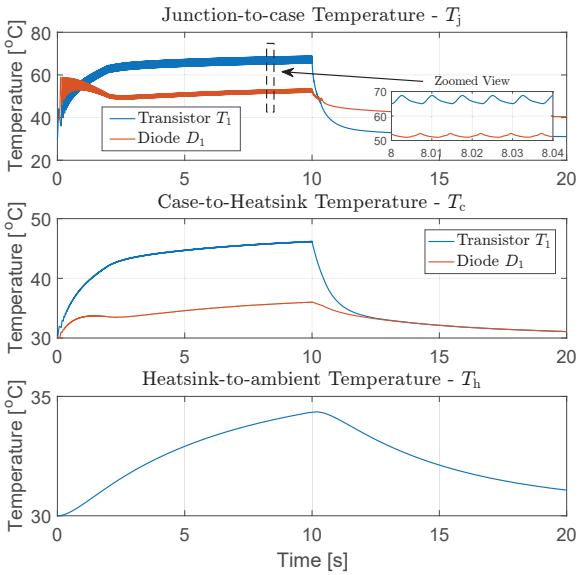

Fig. 9. Power device thermal loading (Component-level mission profiles – Level 4).

C. Component-level mission profile modeling

In order to determine the component-level mission profiles, the converter-level current and voltage loading needs to be introduced into the component-level models, which include the average switching cycle power loss model and the thermal model.

Within the power loss model, the conduction losses of the power devices can be determined based on the conduction voltage (for transistor) and forward voltage (for diode) characteristics, which are provided by the manufacturer in the data sheet.

Similarly, based on the switching energy (for transistor) and reverse recovery energy (for diode) characteristics the switching losses of the semiconductor devices can be calculated. Due to the dependency between the loss characteristics and temperature, the junction temperature (T_j) of the power devices needs to be introduced as feedback from the thermal model. Finally, by adding together the conduction and the switching losses, the total power losses generated by the power devices can be identified. A detailed description of the power loss model and the equations which are used in order to characterize the devices can be found in [16]-[18].

Thus, the total losses generated by the upper transistor and diode, under the given mission profiles, for the motor drive system study case, can be seen in Fig. 8.

In the following, the power device losses can be translated into the corresponding thermal loading. By employing the thermal model proposed in [19], the high dynamics of the junction temperature of the devices can be identified by using a multilevel Foster RC network, while the slow dynamics of the case and heat sink temperatures can be estimated by filtering the power losses through a low-pass filter, respectively, by including the outer thermal network of the IGBT module

(e.g. thermal grease and heat sink). Again, it should be noted that all the necessary parameters for the thermal calculations (e.g. thermal resistance R_{jc}, thermal capacitance C_{jc}, etc.) can normally be found in the device data sheet, or they can be determined by means of experimental test.

By introducing the power losses shown in Fig. 8, into the thermal model, the thermal stress which occurs on the power device is calculated and thus the component-level mission profiles are made available to the user. As it can be observed in Fig. 9, under the assumption that the ambient temperature is constant and equal to 30 ^{o}C, the transistor represents the most stressed component, and thus a faster wear-out is expected.

D. Component-level reliability modeling

Based on the obtained component-level mission profiles, the reliability assessment procedure can be applied in order to estimate the lifetime of the power semiconductor devices.

In order to correctly map the thermal loading data to the strength model, the Rainflow counting algorithm needs to be applied. By employing the counting algorithm the junction and case temperatures of the power devices will be translated into the thermal cycle amplitude (ΔT_j), thermal cycle mean value (T_{mj}), and thermal cycle period (t_{period}). As it has been shown in [20]-[22] all 3 parameters have an impact on the lifespan of the power device.

By introducing the regulated thermal cycles into the Semikron lifetime model [23], the power device damage (consumed B_{10} lifetime) corresponding to the *n*th thermal cycle can be computed according to the following equation [24]:

$$\mathrm{Damage_n} = \frac{100}{\mathrm{N_n}}(\%) \tag{1}$$

where N_n represents the number of thermal cycles with a 10% failure rate (B_{10}). The total accumulated damage that occurs of the power devices can be determined by using Miner's linear accumulation rule [25]

$$\mathrm{Damage} = \sum_{\mathrm{n=1}}^{\mathrm{m}} \mathrm{Damage_n} \tag{2}$$

where $1 \leq n \leq m$ and m represents the total number of thermal cycles resulting from the Rainflow counting algorithm. The resulting accumulated damage which occurs on the power devices during the given mission profiles is shown in Fig. 10.

Based on the power device damage, the lifetime can be estimated according to the following equation:

$$\mathrm{Lifetime} = \frac{\mathrm{Period\ of\ mission\ profile\ (s)}}{\mathrm{Operating\ period\ (s)} \cdot \mathrm{Acc.\ Damage}} \tag{3}$$

Assuming that the motor drive system is operated for 12 hours per day, according to (3), the lifetime estimation for the transistor and diode are approximately 10 years and 40 years, respectively.

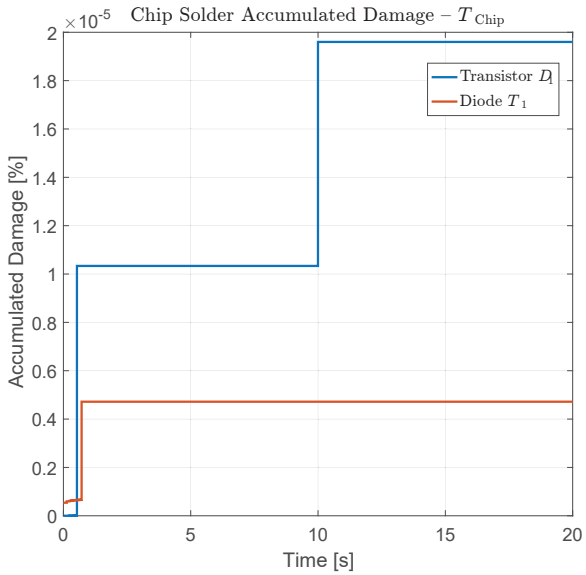

Fig. 10. Power device total accumulated damage.

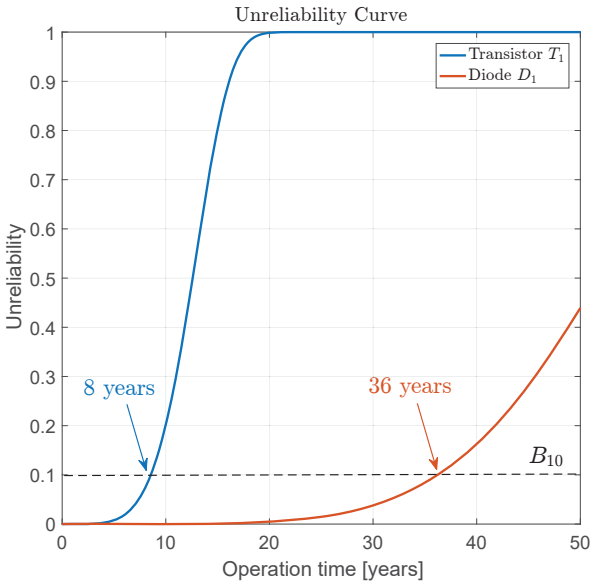

Fig. 11. Unreliability curves for power devices with 5% variations in lifetime model coefficients and stressor.

The final step in the power device reliability assessment procedure is to include and take into consideration the variation and uncertainties which may occur in the lifetime model coefficients and stressor data. The variations in the lifetime model coefficients are introduced in order to compensate for the degree of uncertainty which is derived from the accelerated test results. Similarly, the variations in the stress are introduced because of the uncertainties introduced by the manufacturing process (which may result in junction temperature variations), and by the operating mission profiles of the motor drive system. Thus, a statistical approach based on Monte Carlo

simulation is used in order to investigate the lifetime performance of the power devices, subject to parameter variations [26]-[27].

Assuming a 5% variation in the lifetime model coefficients (A, β_1, β_2, and β_3) and in the thermal stress (ΔT_j, T_{mj}, and t_{period}), the Monte Carlo simulation is performed with 10,000 samples. The resulting unreliability curves for the upper transistor and diode of the machine-side inverter of the motor drive system are shown in Fig. 11, where a decrease of approximately 10% can be noted in the estimated B_{10} lifetime.

E. System-level reliability modeling

Finally, based on the individual reliability performance of the power devices the system-level reliability assessment can be performed. Due to the fact the failures induced by random events are difficult to model and estimate, they will be taken into account as statistical input values. For the given study case the frequency of occurrence for random events is assumed as 1 percent per year.

Additionally, assuming that all 6 transistors and 6 diodes which are included in the IGBT module have a similar reliability performance as the investigated transistor/diode pair (T_1/D_1), the reliability of the power module sub-assembly can be calculated according to the following equation [27]:

$$F_{\text{Sub}}(t) = 1 - \prod(1 - F_{\text{Comp(i)}}(t)) \tag{4}$$

where, F_{Sub} represents the sub-system failure function, and $F_{\text{Comp(i)}}$ represents the individual component failure function.

The results of the Reliability Block Diagram (RBD) analysis are shown in Fig. 12, where it can be seen that the B_{10} lifetime estimation of IGBT power module is of approximately 6 years.

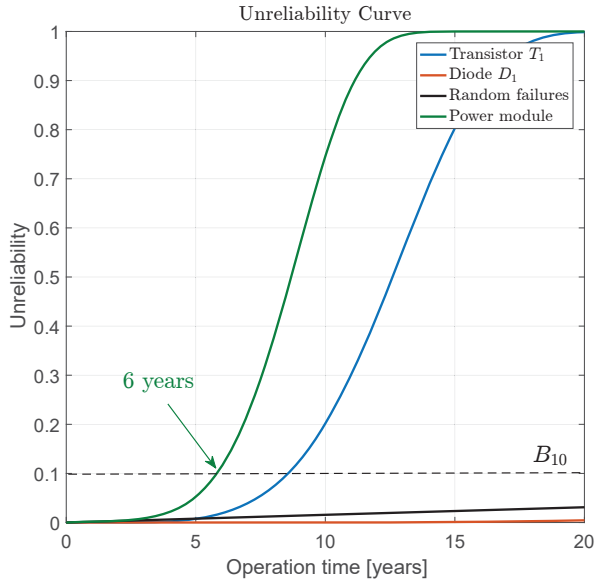

Fig. 12. Unreliability curve for the whole IGBT power module sub-assembly.

IV. Conclusions

In this paper a novel reliability assessment tool (Design for Reliability and Robustness) focused on power electronics systems has been proposed. The main framework and concept of the DfR^2 tool have been introduced, highlighting the main advantages of the tool, among which: user-friendly graphical user interface, modular implementation approach, various mission profile input levels, and fast and straightforward component and system-level reliability assessment. Additionally, in order to validate the implementation and the employed procedures within the tool, a motor drive application study case has been investigated. A brief description of the application mission profile input levels has been presented, and the component-level reliability assessment procedure has been successfully applied to the components of interest (transistor/diode pair). Finally, the reliability assessment of the IGBT power module sub-assembly has been investigated.

References

[1] L. M. Moore, and H. N. Post, "Five years of operating experience at a large utility-scale photovoltaic generating plant," in *Prog. Photovolt.: Res. Appl.*, vol. 16, no. 3, pp. 249 - 259, 2008.

[2] J. B. Gayo, "Reliability focused research on optimizing Wind Energy systems design, operation and maintenance - Tools, proofs of concepts, guidelines & methodologies for a new generation," in *RELIAWIND Project*, 2011.

[3] B. Hahn, M. Durstewitz, and K. Rohrig, "Reliability of wind turbines - Experience of 15 years with 1500 WTs," in *Wind Energy*. Berlin, Germany: Springer, 2007.

[4] S. Faulstich, P. Lyding, B. Hahn, and P. Tavner, "Reliability of offshore turbines - Identifying risks by onshore experience," in *Proc. of EOW*, 2009, pp. 1463 - 1472.

[5] K. J. P. Macken, I. T. Wallace, and M. H. J. Bolleno, "Reliability assessment of motor drives," in *Conf. Res. PESC*, 2006, pp. 1 - 7.

[6] S. Yang, A. Bryant, P. Mawby, D. Xiang, L. Ran, and P. Tav, "An Industry-Based Surveyof Reliability in Power Electronic Converters," *IEEE Trans. on Industry Applications*, vol. 47, no. 3, pp. 1441 - 1451, Jun. 2011.

[7] ZVEI: Die Elektroindustrie, *Handbook for Robustness Validation of Automotive Electrical/Electronic Modules*, German Electrical and Electronics Manufacturer Association, June 2013.

[8] M. H. Bierhoff, and F. W. Fuchs, "Semiconductor losses in voltage source and current source IGBT converters based on analytical derivation," in *Proc. of Power Electronics Specialists Conference*, vol. 4, pp. 2836 - 2842, 2004.

[9] U. M. Choi, *Thesis: Studies on IGBT Module to Improve the Reliability of Power Electronic Systems*. Aalborg: Aalborg University Press, Feb. 2016.

[10] V. Smet, F. Forest, J.-J. Huselstein, F. Richardeau, Z. Khatir, S. Lefebvre, and M. Berkani, "Ageing and Failure Modes of IGBT Modules in High-Temperature

Power Cycling," *IEEE Trans. on Industrial Electronics*, vol. 58, no. 10, pp. 4931 - 4941, Oct. 2011.
[11] "DfR Solutions." Internet: http://www.dfrsolutions.com/, [10 Jul. 2017].
[12] "Center for Advanced Life Cycle Engineering." Internet: http://www.calce.umd.edu/software/, [10 Jul. 2017].
[13] I. Vernica, K. Ma, and F. Blaabjerg, "Optimal derating strategy of power electronics converter for maximum wind energy production with lifetime information of power devices," *J. Emerg. Sel. Topics Power Electron*, vol. 6, no. 1, pp. 1 - 10, Mar. 2018.
[14] I. Vernica, K. Ma, and F. Blaabjerg, "Reliability assessment platform for the power semiconductor devices - Staudy case on 3-phase grid connected inverter application," *Microelectron. Rel.*, vol. 76 - 77, pp. 31 - 37, Sep. 2017.
[15] K. Ma, and F. Blaabjerg, "Multi-timescale modelling for the loading behaviours of power electronics converter," in *Proc. of ECCE*, 2015, pp. 5749 - 5756.
[16] M. Musallam, C. Yin, C. Bailey, and M. Johnson, "Mission profile based reliability design and real-time life consumption estimation in power electronics," *IEEE Trans. on Power Elect.*, vol.30, no.5, pp. 2601-2613, 2015.
[17] A. T. Bryant, P. A. Mawby, P. R. Palmer, E. Santi, and J. L. Hudgins, "Exploration of power device reliability using compact device models and fast electrothermal simulation", *IEEE Trans. on Ind. Appl.*, vol.44, no.3, pp. 894 - 903, Jun. 2008.
[18] K. Ma, A. S. Bahman, S. M. Beczkowski, and F. Blaabjerg, "Complete loss and thermal model of power semiconductors including device rating information," *IEEE Trans. Power Electron.*, vol. 30, no. 5, pp. 2556 - 2569, 2015.
[19] K. Ma, N. He, M. Liserre, and F. Blaabjerg, "Frequency-domain thermal modeling and characterization of power devices," *IEEE Trans. Power Electron.*, vol. 31, no. 10, pp. 7183 - 7193, 2016.
[20] U. Scheuermann, "Reliability challenges of automotive power electronics," *Microelectron. Rel.*, Vol.49, No.9-11, pp.1319-1325, 2009.
[21] U. Scheuermann, R. Schmidt, "A new lifetime model for advanced power modules with sintered chips and optimized Al wire bonds," *Proc. of PCIM*, pp.810-813, 2013.
[22] J. Berner, "Load-cycling capability of HiPak IGBT modules," *ABB Application Note 5SYA 2043-02*, 2012.
[23] A. Wintrich, U. Nicolai, W. Tursky, and T. Reimann, *Semikron: Application Manual Power Semiconductors*, SEMIKRON International GmbH, 2015.
[24] K. Ma, M. Liserre, F. Blaabjerg, and T. Kerekes, "Thermal loading and lifetime estimation for power device considering mission profiles in wind power converter," *IEEE Trans. Power Electron.*, vol. 30, no. 2, pp. 590 - 602, 2015.
[25] M.A. Miner, "Cumulative damage in fatigue", *Journal of Applied Mechanics*, no.12, A159-A164, 1945.
[26] D. Zhou, H. Wang, F. Blaabjerg, S. K. Kaer, and D. Blom-Hansem, "System-level reliability assessment of power stage in fuel cell application," in *Proc. of ECCE*, 2016, pp. 1 - 8.
[27] P. D. T. O'Connor, and A. Kleyner, *Practical Reliability Engineering (fifth edition)*. New York, USA: Wiley, 2012.